THE AMERICAN MINERALOGIST, VOL. 55, SEPTEMBER–OCTOBER, 1970

CRYSTAL FIELD SPECTRA AND EVIDENCE OF CATION ORDERING IN OLIVINE MINERALS[1]

ROGER G. BURNS,[2] *Department of Geology and Mineralogy, University of Oxford, England*

ABSTRACT

Polarized absorption spectral measurements are described of several Mg^{2+}–Fe^{2+} and Fe^{2+}–Mn^{2+} olivines. The spectra contain three overlapping absorption bands in the near infrared originating from electronic transitions within Fe^{2+} ions. The central, more intense band arises from Fe^{2+} in the $M(2)$ positions, whilst the $M(1)$ positions are represented by two broad, outer bands. The relative intensities of the three bands are polarization dependent, indicating that Fe^{2+} olivines are strongly pleochroic in the infrared. The band maxima move to longer wavelengths with increasing iron and manganese contents of the olivine. The compositional variations form determinative curves for Fe_2SiO_4 contents of unanalysed olivines of the forsterite-fayalite series.

Fe^{2+} site populations have been estimated from the areas under the absorption bands. In the forsterite-fayalite series Fe^{2+} ions are evenly distributed over the $M(1)$ and $M(2)$ positions, but there are indications of slight relative enrichments in the $M(2)$ positions of some specimens. Significant cation ordering occurs in the fayalite-tephroite series, in which Fe^{2+} ions are enriched in the $M(1)$ positions as a result of the preference of Mn^{2+} ions for the $M(2)$ positions. The uniform distributions of Fe^{2+} ions in the forsterite-fayalite series are explained by crystal field theory.

INTRODUCTION

Olivines remain one group of ferromagnesian silicate minerals in which cation ordering has not been demonstrated by conventional methods. In the amphibole and pyroxene crystal structures, for example, the evidence of cation ordering from X-ray measurements (Ghose, 1961, 1965) has been substantiated by Mössbauer spectroscopy (Bancroft, Burns and Maddock, 1967a; Bancroft, Burns and Howie, 1967; Ghose and Hafner, 1967) and site population determinations have been made. However, although the olivine structure contains two distinct cation sites, $M(1)$ and $M(2)$, neither X-ray (Hanke, 1965; Birle, Gibbs, Moore and Smith, 1968) nor Mössbauer (Bancroft, Burns and Maddock, 1967b) measurements have been able to detect ordering of Mg^{2+}, Fe^{2+} and Mn^{2+} ions. The lack of success by Mössbauer spectroscopy has been due to the difficulty in resolving contributions to the spectra from Fe^{2+} ions in the $M(1)$ and $M(2)$ positions. In the room-temperature Mössbauer spectra of olivines (Sprenkel-Segel and Hanna, 1964; Bancroft *et al*, 1967b) the

[1] Paper presented at the Eighth International Union of Crystallography Congress, Stony Brook, New York, August 1969 [Abstract published in *Acta Crystallogr.*, **A25,** S59, (1969)].

[2] Present address: Department of Earth and Planetary Sciences, Massachusetts Institute of Technology, Cambridge, Massachusetts 02139.

parameters for iron in the two sites are almost identical.[1] Furthermore, since iron and manganese have similar scattering factors it has been difficult to distinguish between Fe^{2+} and Mn^{2+} ions in silicate structures by X-ray methods.

In the crystal field spectra of olivines, however, contributions from Fe^{2+} ions in the two crystallographic positions can be distinguished. This paper describes polarized absorption spectral measurements on a range of specimens from which it has been possible to estimate site populations in olivines of the forsterite-fayalite series, $(Mg, Fe)_2SiO_4$, and fayalite-tephroite series, $(Fe, Mn)_2SiO_4$.

While no investigation has been published of the compositional variations of the crystal field spectra of olivines, several papers have described absorption spectra of various individual specimens. Thus, room-temperature measurements in the visible and near infrared regions have been made on various forsteritic olivines in unpolarized (Clark, 1957; Grum-Grzhimailo, 1958, 1960; White and Keester, 1966) and polarized (Farrell and Newnham, 1965; Burns, 1965, 1969; Shankland, 1969) light, and of a fayalite in polarized light (Burns, 1965, 1966, 1969). The spectra of olivines at elevated temperatures (Burns, 1965, 1969; Fukao, Mizutani and Uyeda, 1968) and pressures (Balchan and Drickamer, 1959) have also been reported. In addition, the diffuse reflectance spectra of Mn^{2+} in tephroite and glaucochroite have been described (Keester and White, 1968).

Compositional variations of vibrational and rotational bands in the infrared spectra of several olivines of the forsterite-fayalite and fayalite-tephroite series have been measured (Lehmann, Dutz and Koltermann, 1961; Tarte, 1962; Duke and Stephens, 1964). However, no systemmatic studies of the electronic spectra of intermediate Mg^{2+}—Fe^{2+} and Fe^{2+}—Mn^{2+} olivines have been reported so far. This paper, therefore, also describes the compositional variations of the crystal field spectra of various olivine minerals of the forsterite-fayalite and fayalite-tephroite series.

Experimental Methods

Measurements were made on eleven minerals of the forsterite-fayalite series and five minerals of the fayalite-tephroite series. Many of the specimens, which were obtained as

[1] In the Mössbauer spectra of fayalite at elevated temperatures (above 639°K) the outer quadrupole doublet is resolved into two peaks of equal intensity (Eibschütz and Ganiel, 1967). In the low temperature spectra (below 55°K) the hyperfine splitting has been resolved into two sets of lines originating from different Fe^{2+} ions (Kundig, *et al.* 1967). However, these measurements have not been extended to olivines of intermediate compositions and no site population data are yet available.

petrographic thin sections from rock collections at Berkeley, Cambridge and Oxford, had been analyzed previously. The compositions of the remainder were determined by electron microprobe analysis, using Geoscan (analyst, Burns at Cambridge) and MAC 400 (analyst, Dr. D. C. Harris at Ottawa) instruments. The compositions and sources of the olivines are summarized in Table 1. Concentrations are expressed as mole percentages of fayalite (Fe_2SiO_4), tephroite (Mn_2SiO_4) and larnite (Ca_2SiO_4) components. All but two of the Mg^{2+}–Fe^{2+} olivines contain less than three percent Mn_2SiO_4. The compositions of the Fe^{2+}–Mn^{2+} olivines are more variable and the specimens include a picrotephroite with 23.4 percent Mg_2SiO_4 and a roepperite with 8.6 percent Zn_2SiO_4 and 8.4 percent Mg_2SiO_4.

Spectra were measured over the range 4000–22000 Å in polarized light by a microscope technique (Burns, 1966). A thin section (0.003–0.05 cm) cut from rock containing the olivine or from a single crystal and mounted in Canada balsam, was placed on a three-axis universal stage mounted on a polarizing microscope with calcite Nicol polarizers. A single crystal of the olivine was brought into the field of view of the microscope and a suitable vibration or crystallographic axis was oriented E-W to coincide with the polarization of the lower Nicol. The microscope was then mounted in the sample beam of a Cary model 14 recording spectrophotometer. An identical microscope system holding a glass slide and Canada balsam was placed in the reference beam.

All three polarized spectra corresponding to light vibrating along the α, β and γ axes were measured. Since olivine belongs to the orthorhombic system (space group *Pbnm*), vibration and crystallographic axes coincide with $\alpha=b$, $\beta=c$ and $\gamma=a$[1] The γ spectra contain intense absorption bands and could be measured conveniently on conventional petrographic thin sections. However, absorption bands in the α and β spectra are weak, especially in forsteritic olivines, and thick sections or mounted plates had to be used to record these spectra.

The Cary spectrophotometer plots the spectrum on a chart recorder, which registers the optical density (log I_0/I) at each wavelength.[2] In order to resolve overlapping bands it is necessary first to replot the spectra on a wavenumber (cm.$^{-1}$) scale.

The spectra of olivines were found to consist of overlapping absorption bands. These were resolved into component Gaussian curves in the optical density/wavenumber spectra by means of a Dupont model 310 curve resolved. This instrument also computes the area ratios of the component Gaussian curves.

The Olivine Crystal Structure

The structure of olivine has been described by several crystallographers (Bragg and Brown, 1926; Belov, Belova, Andrianova and Smirnova, 1961; Hanke and Zeeman, 1963; Gibbs, Moore and Smith, 1963; Hanke, 1965; Birle, Gibbs, Moore and Smith, 1968). The crystal structure of fayalite (Birle *et al* 1968) consists of independent SiO_4 tetrahedra linked by divalent cations in six-fold coordination. There are two non-equivalent six-coordinate positions in the structure, which are designated

[1] This orientation differs from that of Farrell and Newnham (1965) who referred their spectra to the alternative space group setting *Pnma*. In this setting, $\alpha=a$, $\beta=b$ and $\gamma=c$.

[2] $\log I_0/I=\epsilon ct=$ optical density (O.D.) where I_0 and I are the intensities of the incident and transmitted beams, respectively; c is the concentration of the absorbing species (moles per liter or gm. ions per liter); t is the thickness of the sample (cm.); and ϵ is the molar extinction coefficient (liter mole $^{-1}$ cm.$^{-1}$).

TABLE 1. COMPOSITIONS AND SOURCES OF THE OLIVINE SPECIMENS

	1	2	3	4	5	6	7	8	9	10	11	12	13	14	15	16
SiO_2	n.d.	39.4	n.d.	35.59	33.2	32.47	31.4	30.42	30.3	29.5	28.3	30.0	29.35	29.6	n.d.	29.31
FeO	8.2	11.8	14.9	36.18	45.7	53.14	54.9	57.62	62.0	68.0	67.9	49.5	30.3	22.15	0.09	1.67
MnO	0.15	0.2	0.15	0.45	4.95	0.73	5.3	n.d.	1.15	2.1	1.0	18.6	29.4	47.0	55.65	65.62
MgO	50.1	46.9	43.6	26.80	16.0	13.22	8.7	8.17	5.5	0.2	0	1.85	3.45	0.5	10.75	0.71
CaO	0.04	0.4	0.21	0.02	0.1	0	0.1	1.32	0.1	0.2	0.3	0.1	0.25	0.5	1.10	0.70
NiO	0.41	n.d.	0.33	n.d.	n.d.	n.d.	n.d.	n.d.	0	n.d.	0	n.d.	n.d.	n.d.	n.d.	n.d.
ZnO	n.d.	n.d.	n.d.	n.d.	n.d.	n.d.	0	n.d.	0	n.d.	0.1	n.d.	7.10	n.d.	0	n.d.
others	—	—	—	0.51	—	0.54	—	1.70	0.1	—	0.1	—	—	—	—	—
total	—	98.7	—	99.55	99.95	100.10	100.4	99.62	99.1	100.0	97.7	100.05	99.85	99.75	—	98.01
Fe_2SiO_4	8.4	12.3	16.1	42.9	57.5	70.3	72.4	78.0	85.1	96.1	97.9	69.0	41.5	31.1	0.1	1.0
Mg_2SiO_4	91.5	87.0	83.5	56.6	35.9	28.5	20.4	20.0	13.3	0.5	0.0	4.6	8.4	1.3	23.4	4.2
Mn_2SiO_4	0.1	0.2	0.2	0.5	6.35	1.0	7.1	—	1.3	3.0	1.4	26.2	41.0	66.8	74.5	93.7
Ca_2SiO_4	0.0	0.5	0.2	0.0	0.15	0.1	0.2	2.0	0.2	0.4	0.6	0.2	0.4	0.9	1.8	1.2
Zn_2SiO_4	—	—	—	—	—	—	0	—	0	—	—	—	8.6	—	0	—

1. Forsterite (Berkeley 618-181-2), Kauai, Hawaii (White, 1965)
2. Chrysolite (Berkeley 12489), Yan Mayan (analyst: Burns)
3. Chrysolite (Berkeley 618-254-2), Hualalai, Hawaii (White, 1965)
4. Hyalosiderite (Oxford 5112), Skaergaard intrusion, East Greenland (Vincent, Douglas and Bown, 1964)
5. Hortonolite (Berkeley 12494), location unknown (analyst: Burns)
6. Ferrohortonolite (Oxford 5181), Skaergaard intrusion, East Greenland (Vincent, Douglas and Bown, 1964)
7. Ferrohortonolite (Berkeley 12495), location unknown (analyst: Harris)
8. Ferrohortonolite (Cambridge), Beaver Bay, Minnesota (Muir, 1954; Deer, Howie and Zussman, 1963, v.1., p. 13)
9. Ferrohortonolite (Oxford 4146), Skaergaard intrusion, East Greenland (Smith, 1966)
10. Fayalite (AMNH 10927), Cape Anne, Massachusetts (analyst: Burns)
11. Fayalite (Oxford 4139), Skaergaard intrusion, East Greenland (Smith, 1966)
12. Knebelite (Berkeley 12511), Schisshyttan, Sweden (analyst: Harris)
13. Roepperite (Bauer collection, Harvard), Franklin, New Jersey (analyst: Harris)
14. Tephroite, Broken Hill, Australia (analyst: Harris)
15. Picrotephroite (Harvard 106580), Långban, Sweden (Hurlbut, 1961)
16. Tephroite, Clark Peninsula, Antarctica (Mason, 1959; Deer, Howie and Zussman, 1963, v.l., p. 37).

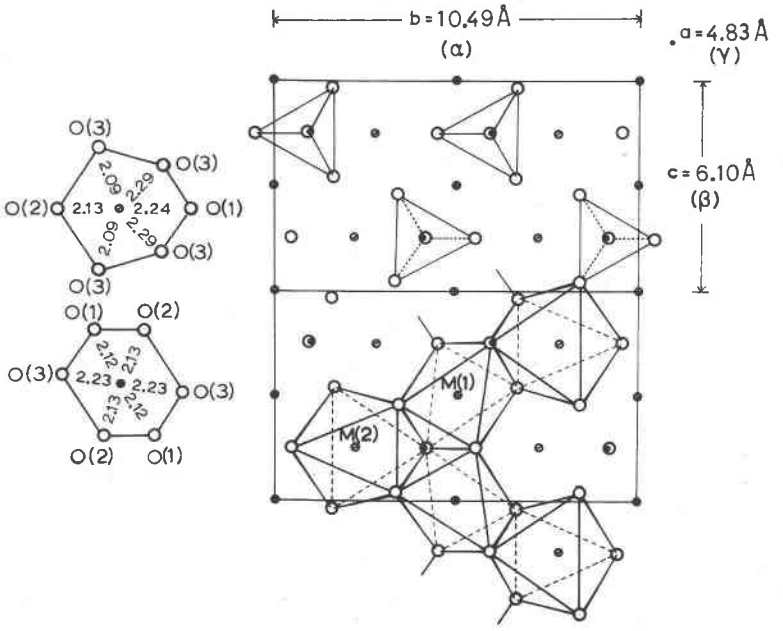

FIG. 1. The olivine crystal structure. This (100) projection of the fayalite structure shows oxygen coordination polyhedra about cation positions at $x=0.5$. The figure shows a chain of linked octahedra extending along the c axis. Metal-oxygen distances in each coordination site are indicated. ⊕ M(1); ∅ M(2); ○ oxygen; · silicon.

by $M(1)$ and $M(2)$.[1] Both coordination sites are distorted from octahedral symmetry (Fig. 1.). The configuration of the six nearest oxygen atoms surrounding the $M(1)$ position is that of an axially elongated octahedron with a rhomboid median plane, in which the cation is centrally located. Although the point symmetry of the $M(1)$ position is $\bar{1}$ (C_i), the local symmetry of the $M(1)$ coordination site is approximately $4/mmm(D_{4h})$ with the tetrad axis through O(3)—$M(1)$—O(3). The oxygen coordination polyhedron about the $M(2)$ position is irregular and the point symmetry is $m(C_s)$. However, the local symmetry of the $M(2)$ coordination site may be regarded as approximately $3m$ (C_{3v}) with the triad axis parallel to a. A cation in the $M(2)$ position does not lie at the center of symmetry of the coordination site, and is offset along b. A significant feature of the olivine structure is the infinite bands of

[1] The symbolism $M(1)$ and $M(2)$ follows that originally proposed by Bragg and Brown (1926), who used Mg(I) and Mg(II). Hanke (1965) used the alternative symbols A_i and A_m for the $M(1)$ and $M(2)$ sites, respectively, to distinguish between the two positions with inversion ($\bar{1}$) and mirror plane (m) point symmetries.

cations which extend along the *c* axis. The structure of a forsterite with 10 percent Fe_2SiO_4 is similar (Birle *et al*, 1968). Each metal-oxygen distance is shorter and the mean distances are reduced from 2.16 Å ($M(1)$ site) and 2.19 Å ($M(2)$ site) in fayalite to 2.10 Å ($M(1)$ site) and 2.14 Å ($M(2)$ site) in forsterite (Hanke, 1965; Birle, *et al*,. 1968).

No crystal structure determination of a tephroite has been reported. It is generally inferred from X-ray powder and rotation photographs that tephroite and fayalite are isostructural (O'Daniel and Tscheischwilli, 1944; Deer, Howie and Zussman, 1963, vol. 1, 35). Neutron diffraction experiments on Fe_2SiO_4 and Mn_2SiO_4 have shown that the magnetic and chemical unit cells are identical (Santoro, Newnham and Nomura, 1966). No information is available on the configuration of the oxygen atoms about the $M(1)$ and $M(2)$ positions or extent of ordering of Mn^{2+} and Fe^{2+} ions in the structure. Cell parameters indicate that the metal-oxygen distances are larger in the structures of manganiferous olivines. Although Mn^{2+} ions are predicted to favor the larger $M(2)$ coordination site (Ghose, 1962), the similar scattering factors of iron and manganese make it difficult to detect Mn^{2+}—Fe^{2+} ordering in the olivine structure by X-ray methods. However, the detection of Mn^{2+}—Fe^{2+} ordering is now possible using counter data and available site refinement programs (Brown and Gibbs, personal communication).

Results: Spectra of the Forsterite-Fayalite Series

The polarized spectra of olivines of the forsterite-fayalite series have been illustrated several times previously (Burns, 1965; Farrell and Newnham, 1965; Burns 1969, 1970). However, a typical set of spectra of fayalite (specimen 10) taken from the chart recorder of a Cary spectrophotometer are shown in Figure 2. The unresolved polarized spectra of Mg^{2+}—Fe^{2+} olivines display the following features:

1. Each polarized spectrum of a given olivine is distinctive. Thus, olivines of the forsterite-fayalite series are strongly pleochroic, although the pleochroism is not seen except in fayalite ($\alpha = \gamma =$ pale yellow, $\beta =$ orange yellow) because the principal absorption bands are located outside the visible region (4000–7000 Å).

2. The β spectra consist of two broad bands in the near infrared at 8450–9050 Å and 11000–12400 Å.

3. The α spectra are similar to the β spectra but the maxima centered at 8550–9150 Å occur at slightly longer wavelengths in each spectrum. The maxima at about 12800 Å in the α spectrum of fayalite is not as well developed as the corresponding band in the β spectra, and appears only as a prominent inflexion in the forsterite spectra.

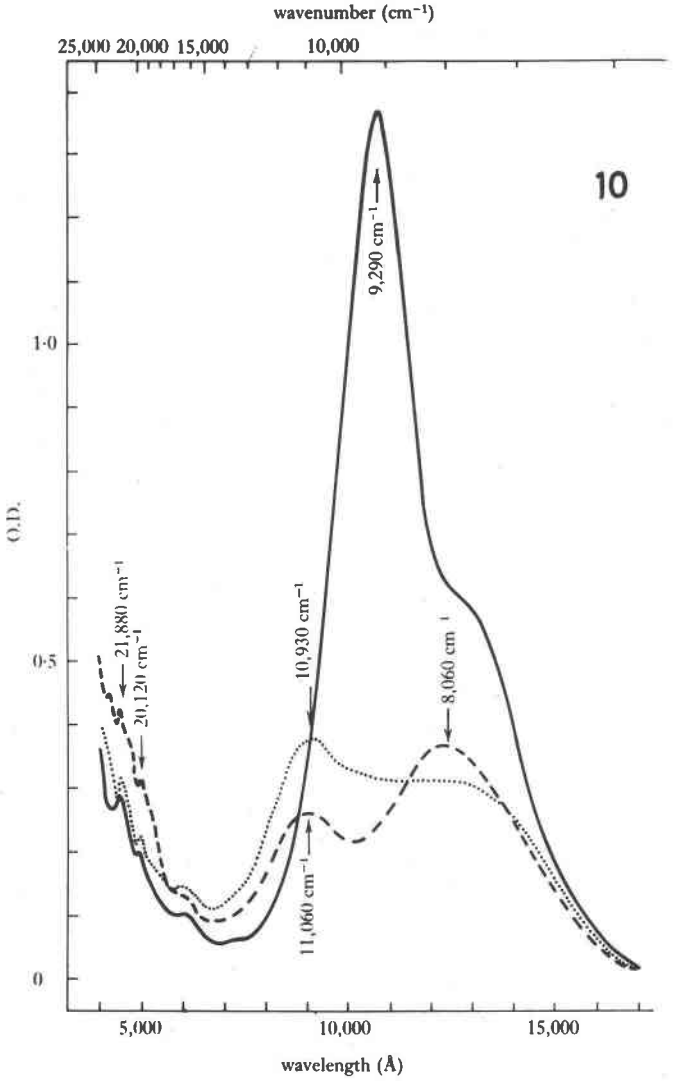

FIG. 2. Polarized absorption spectra of fayalite (specimen 10) · · · α spectrum; --- β spectrum; —— γ spectrum. (optic orientation: $\alpha = b$; $\beta = c$; $\gamma = a$.

4. The γ spectra are three to five times more intense than the α and β spectra, and appear to consist of three overlapping absorption bands, the most intense of which has an absorption maximum at 10400–10800 Å.

5. The absorption edge of an intense charge transfer band located in the ultraviolet region appears below about 5000 Å. It is most conspicuous

TABLE 2. BAND POSITIONS IN THE POLARIZED ABSORPTION SPECTRA OF OLIVINES IN THE NEAR INFRARED

Specimen Number	Mole % Fe_2SiO_4	α spectrum Band I		β spectrum Band I		β spectrum Band III		γ spectrum Band II	
		Å	cm^{-1}	Å	cm^{-1}	Å	cm^{-1}	Å	cm^{-1}
1	8.4	8560	11680	8480	11790	10870	9200	10460	9560
2	12.3	8560	11680	8480	11790	11000	9090	10450	9570
3	16.1	8625	11600	8510	11750	11050	9050	10460	9560
4	42.9	8770	11400	8660	11550	11490	8700	10520	9510
5	57.5	8950	11230	8810	11350	11860	8430	10670	9370
6	70.3	8930	11200	8850	11300	11980	8350	10590	9440
7	72.4	9010	11100	8940	11200	12120	8250	10640	9400
8	78.0	9010	11100	8890	11250	11900	8400	10640	9400
9	85.1	9090	11000	9010	11100	12120	8250	10670	9370
10	96.1	9150	10930	9040	11060	12400	8065	10780	9280
11	97.9	9150	10930	9050	11050	12390	8070	10750	9300
12	69.0	8620	11600	8510	11750	11900	8400	10910	9160
13	41.5	8740	11450	8640	11570	12050	8300	11050	9050
14	31.1	9210	11390	9100	10990	12180	8210	11200	8930

in the spectra of fayalites and extends further into the visible region in the β spectra than it does in the α and γ spectra. This absorption edge produces the optical pleochroism of fayalite.

6. Several weak inflexions and sharp peaks, notably at 4500–4590 Å, 4850–4970 Å and 6100–6300 Å are located on the flanks of the charge transfer band in each polarized spectrum.

7. The absorption maxima of all bands and peaks, together with the absorption edge, migrate to longer wavelengths (smaller energies) with increasing Fe_2SiO_4 component (Table 2.). These shifts show linear trends when absorption maxima expressed in energy units (wavenumbers) are plotted against mole percent Fe_2SiO_4 in the olivine (Figure 3.). The degree of scatter of points about straight lines is most pronounced for olivines with appreciable Mn_2SiO_4 contents (specimens 5 and 7). The plots in Figure 3 could be used as semiquantitative determinative curves for Fe_2SiO_4 contents of unanalysed Mg^{2+}—Fe^{2+} olivines.

In order to resolve the overlapping absorption bands, the three polarized spectra of each olivine were plotted on a wavenumber abscissa scale and component Gaussian curves were located with a Dupont curve resolver. The resolved spectra of three olivines (specimens 2, 5 and 11) are shown in Figure 4.

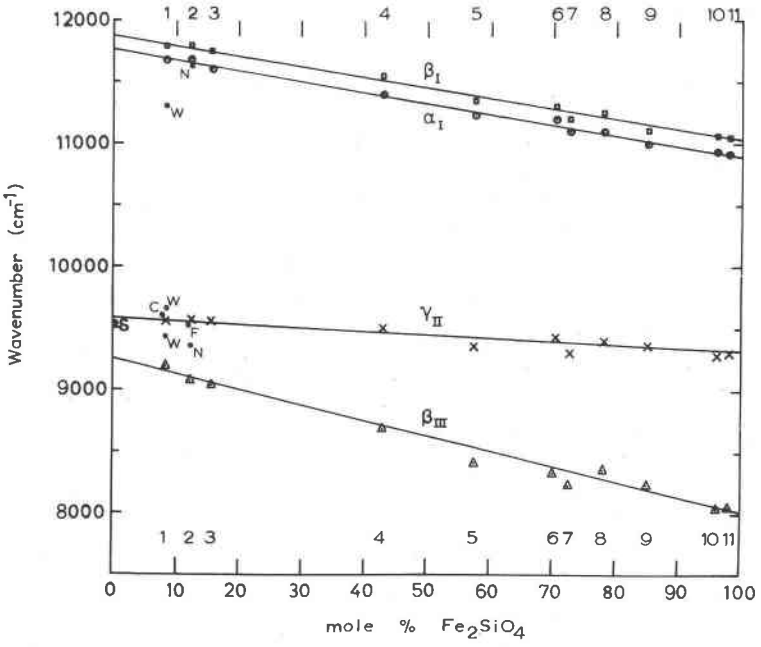

FIG. 3. Compositional variations of absorption maxima in the polarized spectra of Mg^{2+}–Fe^{2+} olivines. ⊡ β spectra (8450–9050 Å); ⊙ α spectra (8550–9150 Å); × γ spectra (10400–10800 Å); △ β spectra (11000–12400 Å); • published data for other forsteritic olivines. C Clark (1957); N Farrell and Newnham (1965); W White and Keester (1966); F Fukao *et al* (1968) S Shankland (1969).

Three component bands, each with a different width at half height, may be resolved in each polarized spectrum. For a given olivine the positions and widths of each band are almost identical in the three polarized spectra, but the relative intensities differ from one spectrum to another. Absorption maxima of each absorption band again decrease linearly with increasing Fe_2SiO_4 content, but the half-widths of corresponding bands remain approximately constant over the composition range. The characteristic properties of the three component bands are:

band I: position 11800–11000 cm^{-1}; half-width 2900 ± 200 cm^{-1}
band II: position 9550–9250 cm^{-1}; half-width 1500 ± 100 cm^{-1}
band III: position 8700–8000 cm^{-1}; half-width 1900 ± 150 cm^{-1}

All three bands contribute appreciably to the γ polarized spectra, with the greatest contribution coming from band II. In fayalite, for example, the areas under the Gaussian curves are in the ratio band I:band II: band III = 23.5:44.0; 32.5 percent. Relatively small deviations from

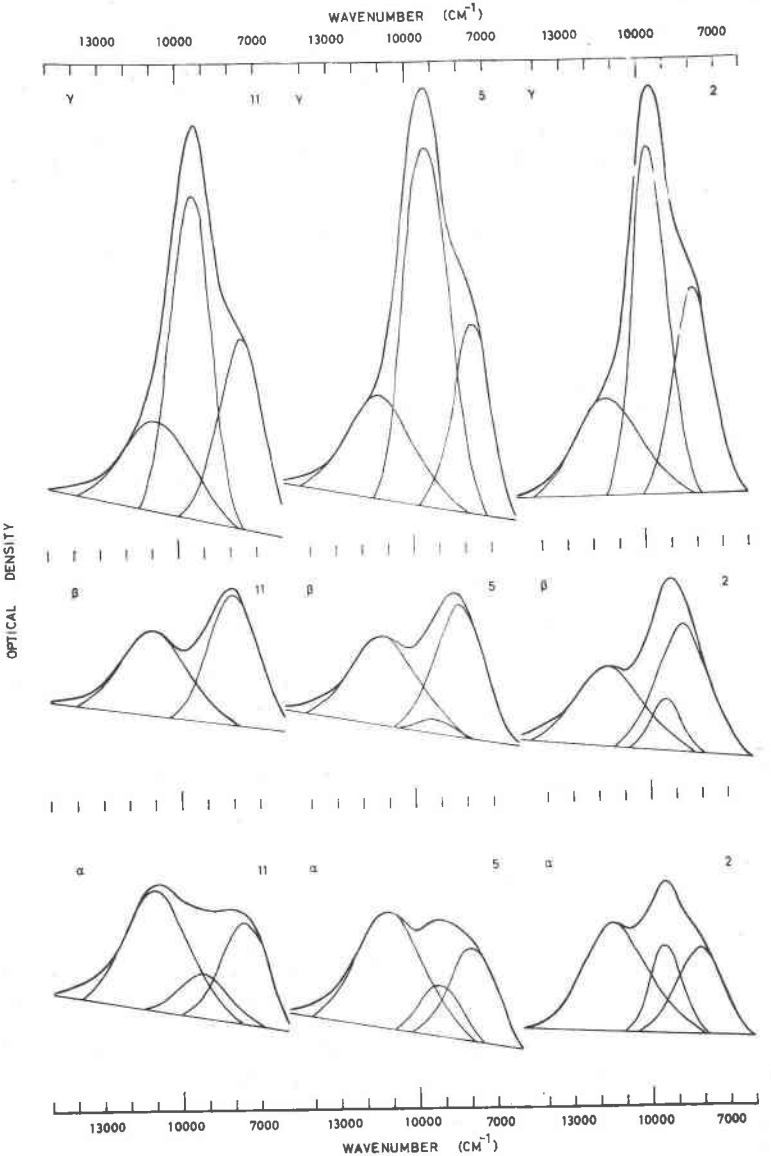

FIG. 4. The polarized absorption spectra of olivines resolved into component Gaussian-shaped bands. The figure shows each polarized spectrum of three olivines (specimens 11, 5 and 2) separated with a Dupont model 310 curve resolver into three overlapping absorption bands.

these values are found in the resolved γ spectra of other Mg^{2+}—Fe^{2+} olivines (Table 4). In the α spectra bands I and III contribute most strongly to the spectra, but a significant contribution comes from band II. With decreasing Fe_2SiO_4 concentration, the contribution from band II increases while the ratio of intensities of band I to band III remains approximately constant. The β spectrum of fayalite contains contributions from bands I and III only. However, again there is an increasing contribution from band II with decreasing Fe_2SiO_4 concentration while the area ratio of band I to band III is approximately constant.

Interpretation of the Spectra. Magnetic susceptibility measurements (Nagata, Yukutake and Uyeda, 1957; Kondo and Miyahara, 1963; Santoro, Newnham and Nomura, 1966) indicate that Fe^{2+} ions in the olivine structure have the high-spin configuration with four unpaired electrons. This would lead to the degenerate $^5T_{2g}$ ground-state and ^5E_g excited state if Fe^{2+} ions were in regular octahedral coordination. However, in the distorted six-coordinate sites of the olivine structure the degeneracies of these crystal field states are resolved. In the $M(1)$ site, which for illustrative purposes is assumed to have approximately D_{4h} symmetry, the octahedral $^5T_{2g}$ ground-state of Fe^{2+} is resolved into the lower ^5E_g state and upper $^5B_{2g}$ state, while the octahedral ^5E_g excited state is resolved into the $^5A_{1g}$ and $^5B_{1g}$ states. In the $M(2)$ site, which may be conveniently approximated to C_{3v} symmetry, the ground-state is $^5A_1$ and there are two excited states with ^5E symmetry. The crystal field states and electronic configurations of the ground states of the Fe^{2+} ion in symmetry D_{4h} and C_{3v} crystal fields are shown in Figure 5.

The intense band at 10400–10800 Å in the γ spectra (band II) is indicative of Fe^{2+} ions in a noncentrosymmetric environment, and originates from a transition to the highest energy state of Fe^{2+} ions in the $M(2)$ positions. This transition is analogous to the $^5A_1 \rightarrow {}^5E$ (upper) transition in a symmetry C_{3v} site (Figure 5f). The bands at 8450–9150 Å (band I) and 11000–12800 Å (band III) represent transitions to the two high energy excited states of Fe^{2+} ions located in the $M(1)$ positions. These transitions are analogous to the $^5E_g \rightarrow {}^5B_{1g}$ and $^5E_g \rightarrow {}^5A_{1g}$ transitions in a symmetry D_{4h} environment (Figure 5e). The transitions $^5A_1 \rightarrow {}^5E$ (lower) and $^5E_g \rightarrow {}^5B_{2g}$ for Fe^{2+} in symmetry C_{3v} and D_{4h} environments, respectively, would be excepted to lie in the far infrared. Absorption bands representing analogous transitions in Fe^{2+} in olivine were not observed in the spectral range measured in this work, but one or other may account for the absorption band at 1670 $cm.^{-1}$ reported by White and Keester (1967).

Confirmation of the assignment of absorption bands in the olivine

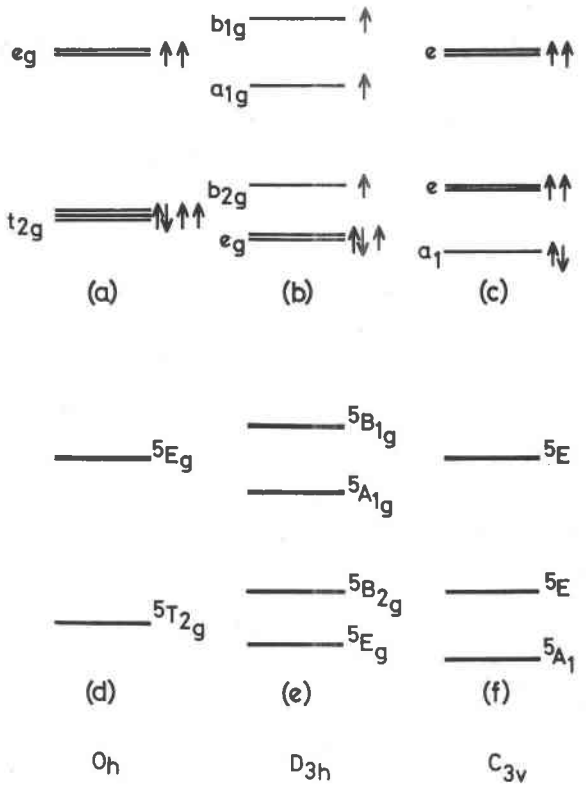

FIG. 5. Energy level diagrams for electronic states and 3*d* orbitals of Fe^{2+} in octahedral, tetragonal and trigonal coordination sites. (a), (b), (c) electronic configurations of the ground-states in sites with symmetry O_h, D_{4h} (elongated along the tetrad axis) and C_{3v} (compressed along the triad axis). (d), (e), (f) crystal field states corresponding to the ground-states shown in (a), (b), and (c), respectively.

spectra stems from spectral measurements of the iron-rich monticellite kirschsteinite, Ca(Mg, Fe)SiO_4, containing 69.4 mole percent $CaFeSiO_4$ (Sahama and Hytönen, 1957). A low intensity, asymmetric absorption band is observed in all three polarized spectra and there is a conspicuous absence of an intense band at about 10800 Å in the γ spectrum. (Burns, 1965). Since Ca^{2+} ions completely fill the $M(2)$ positions in the monticellite structure (Brown and West, 1927; Hanke, 1965; Onken, 1965), the spectra can only arise from absorption by Fe^{2+} ions in $M(1)$ positions. Therefore, the absence of Fe^{2+} ions in $M(2)$ positions can be correlated with the nonappearance of an intense absorption band around 10800 Å in the γ spectrum of kirschsteinite.

TABLE 3. POSITIONS AND ASSIGNMENTS OF SPIN-FORBIDDEN PEAKS (IN Å)

Specimen Number	% Mn_2SiO_4	Positions of Peaks (Å)							
		1	2	3	4	5	6	7	8
2	0.2	6300	(5200)	4850	(4700)	4500	—	—	—
10	3.0	6100	(5250)	4970	(4730)	4590	—	—	(4060)
12	26.2	6350	(5300)	5000	—	4550	(6000)	(4550)	4095
13	41.0	—	—	4950	—	—	6000	4475	4110
14	66.8	—	—	5000	—	—	5900	4400	4100
15	74.5	—	—	—	—	—	5820	4400	4125
16	93.7	—	—	—	—	—	5860	4410	4130
ref. (a)	—	6400	(5250)	4900	4750	4550	—	—	—
ref. (b)	90	—	—	—	—	—	5755	4410	4060
Assignment:									
Fe^{2+}		$^3T_{1g}$	$^3T_{2g}$	$^3T_{1g}$	$^3T_{2g}$	^3E_g	—	—	—
Mn^{2+}		—	—	—	—	—	$^4T_{1g}$	$^4T_{2g}$	$^4A_{1g}$, ^4E_g

Ref. (a) Farrell and Newnham (1965)
Ref. (b) Keester and White (1968)
Unresolved shoulders are bracketed.

The weak peaks located in the visible region of each polarized spectrum of Mg^{2+}—Fe^{2+} olivines represent spin-forbidden transitions within Fe^{2+} ions. An assignment of these peaks, based on that given by Furlani (1957) for similar peaks in the spectra of hydrated Fe^{2+} compounds, is included in Table 3.

The displacement of absorption maxima of bands I, II and III to longer wavelengths with increasing iron content of the olivine may be attributed to the increased unit cell dimensions resulting from the replacement of smaller Mg^{2+} ions by larger Fe^{2+} ions in the olivine structure.

Color and Pleochroism of Olivines. Forsteritic olivines are generally colorless or pale green in thin section. Fayalites display faint optical pleochroism, with $\alpha = \gamma =$ pale yellow and $\beta =$ orange yellow. The spectra illustrated in Figures 2 and 4, however, show that all olivines of the forsterite-fayalite series are distinctly pleochroic beyond the visible region.

The pale green color of olivines arises from absorption of the red portion of the visible region by shoulders of the bands with maxima in the near infrared. The cause of the orange-yellow color of fayalite in β

polarized light is the appearance into the visible region of a charge transfer band located in the ultraviolet. The edge of this band covers more of the blue region in β polarized light than similar bands in α and γ polarized light. As a result, fayalite appears "redder" in β polarized light.

Pleochroism in fayalite results from charge transfer or electronic transitions *between* neighboring ions in the structure. The β indicatrix axis coincides with the c axis along which bands of cations in $M(1)$ and $M(2)$ positions extend throughout the olivine structure (Figure 1). Interatomic distances between ions in adjacent $M(1)$ positions in fayalite are 3.05 Å and $M(1)$–$M(2)$ distances are about 3.20 Å. Although the $M(1)$–$M(2)$ direction does not coincide with the β axis, it does lie in

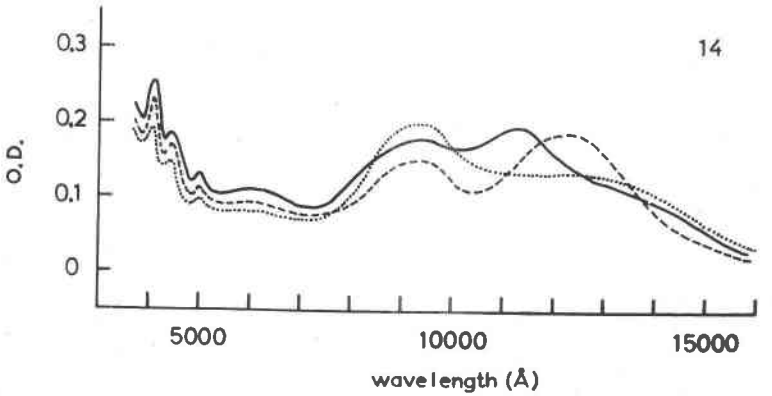

FIG. 6. Polarized absorption spectra of a ferroan tephroite (specimen 14). ··· α spectrum; --- β spectrum; —— γ spectrum; (optic orientation: $\alpha=b$; $\beta=c$; $\gamma=a$).

the (100) plane containing the β axis and infinite bands of cations (Fig. 1). Overlap of t_{2g}-type orbitals of adjacent Fe^{2+} ions situated in $M(1)$ positions along the β axis and between Fe^{2+} ions in adjacent $M(1)$ and $M(2)$ positions in the planes containing the β axis and the bands of cations leads to facilitated charge transfer in β polarized light. In this orientation the electric vector of polarized light is most favorably aligned to induce electron transfer through overlapping t_{2g}-type orbitals of neighboring cations along the chains.

RESULTS: SPECTRA OF THE FAYALITE-TEPHROITE SERIES

The three polarized spectra of the tephroite $(Fe_{0.622}Mn_{1.336}Ca_{0.018}Mg_{0.026})SiO_4$ (specimen 14) are shown in Figure 6, and in Figure 7 the γ spectra of a suite of olivines of the fayalite-tephroite series are illustrated. In contrast to the forsterite-fayalite series, the polarized spectra of man-

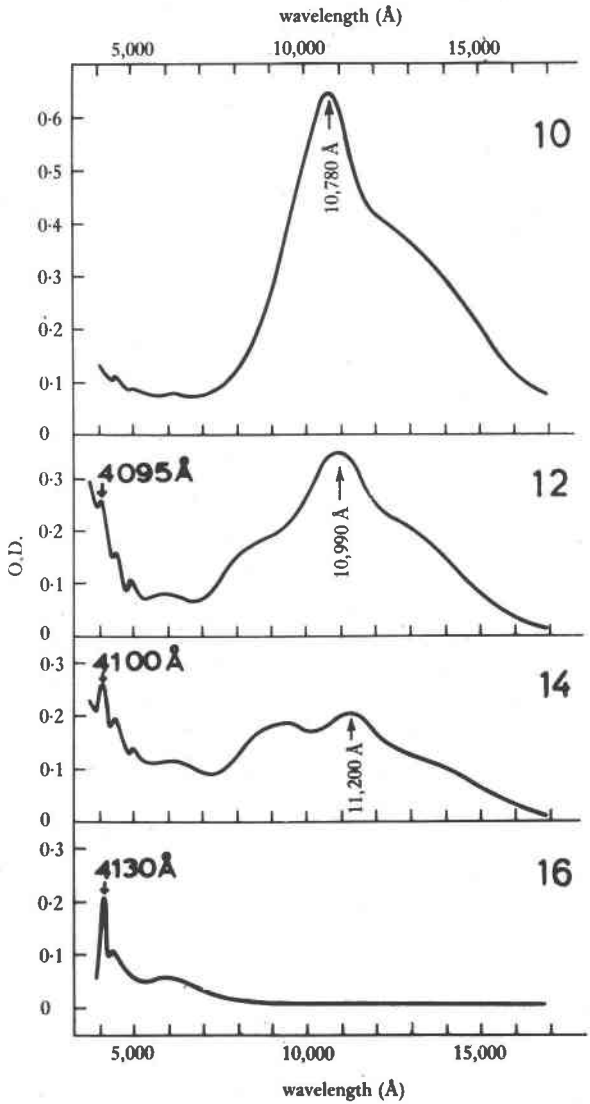

FIG. 7. Polarized absorption spectra of Fe^{2+}–Mn^{2+} olivines. The figure illustrates variations in the γ spectra of specimens 10, 12, 14, and 16 with decreasing Fe_2SiO_4 and increasing Mn_2SiO_4 components.

ganiferous olivines show appreciable compositional variation. In the α and β spectra bands I and III are located at shorter wavelengths in knebelite (specimen 12) than in fayalite (Table 2). In general, the

maxima of bands I and III move to longer wavelengths with increasing Mn_2SiO_4 content. There is also a smaller contribution from band II to the spectra than in Mg^{2+}–Fe^{2+} olivines of similar Fe_2SiO_4 content.

The γ spectra illustrated in Figure 7 display the most pronounced compositional variations:

1. The intense band located at 10780 Å in fayalite migrates to longer wavelengths with deceasing Fe_2SiO_4 component in the manganiferous olivine.

2. With decreasing Fe_2SiO_4 content, the intensity of band II at 10780 Å decreases relative to bands I and III.

3. The weak, sharp peaks at 4520–4550 Å, 4950–5000 Å and 6300–6350 Å originating from spin-forbidden transitions in Fe^{2+} ions, decrease in intensity and move to longer wavelengths with decreasing Fe_2SiO_4 component (Table 3). Additional weak peaks appear at 4095–4130 Å, 4475–4400 Å and 5820–6000 Å and gain intensity with increasing Mn_2SiO_4 content. There is a measurable shift of the peak at 4095–4130 Å to longer wavelengths with increasing Mn_2SiO_4 component (Table 3 and Figure 7)

4. Each of the three polarized spectra of picrotephroite (specimen 15) and pure tephroite (specimen 16) is almost identical: the peaks occur at the same positions in each spectrum, and their relative intensities are approximately the same. The spectra, therefore, conform with the observation that tephroites are nonpleochroic. There is close agreement between the polarized spectrum illustrated in Figure 7d and the diffuse reflectance spectrum of tephroite described by Keester and White (1968).

Interpretation of the Spectra. By comparison with the spectra of fayalite (Figure 2), the peaks at 4520–4550 Å, 4950–5000 Å and 6300–6350 Å, in addition to the broad bands in the infrared (8000–13500 Å), arise from transitions within Fe^{2+} ions. The peaks at 4095–4130 Å, 4475–4400 Å and 5820–6000 Å are due to transitions within Mn^{2+} ions.

The Mn^{2+} ion, which is paramagnetic in olivine (Santoro, Newham and Nomura, 1966) with five unpaired electrons at room temperature, gives rise to the non-degenerate $^6A_{1g}$ ground-state in an octahedral crystal field. This state is not resolved into further states in fields of lower symmetry, such as those in the $M(1)$ and $M(2)$ coordination sites of the olivine structure. Excited states of the Mn^{2+} ions include the $^4T_{1g}$, $^4T_{2g}$, ^4E_g, and $^4A_{1g}$ states, which have lower spin multiplicities than the $^6A_{1g}$ ground-state. Thus, electronic transitions in Mn^{2+} ions are spin-forbidden and lead to weak absorption bands. The peaks in the spectra of manganiferous olivines may be assigned as follows (Table 3):

5820–6000 Å, to ${}^6A_{1g} \rightarrow {}^4T_{1g}$
4475–4400 Å, to ${}^6A_{1g} \rightarrow {}^4T_{2g}$
4095–4130 Å, to ${}^6A_{1g} \rightarrow {}^4E_g, {}^4A_{1g}$

There is no resolution of the transition doublet ${}^6A_{1g} \rightarrow {}^4E_g, {}^4A_{1g}$ in the spectra of manganiferous olivines such as that observed in the polarized spectra of Fe^{3+} ions in epidote (Burns and Strens, 1967).

The γ spectra show that there is a pronounced decrease in relative intensity of band II centered at 10780–11200 Å with increasing Mn_2SiO_4 component in the olivine. Since this band originates from absorption by Fe^{2+} ions in the noncentrosymmetric $M(2)$ site, the spectra of manganiferous olivines show that Mn^{2+} ions selectively replace Fe^{2+} ions in $M(2)$ positions. As a result, Fe^{2+} ions are enriched in the $M(1)$ positions.

On the assumption that the configuration of the $M(1)$ site has approximately D_{4h} symmetry, the displacement of bands I and III to lower wavelengths (higher energies) relative to fayalite might suggest that the mean metal-oxygen distance in the $M(1)$ site is smaller in manganiferous olivines than in fayalite. Furthermore, the increased separation between bands I and III in knebelite (specimen 12) and roepperite (specimen 13) compared to fayalite might suggest that there is increased (tetragonal) distortion of the oxygen coordination polyhedron about the $M(1)$ position in manganiferous and zincian olivines. However, these deductions do not conform with recent structural refinements of manganiferous olivines. Gibbs and Brown (personal communication) find that the mean $M(1)$–O distance in the knebelite $(Fe_{0.514}Mn_{0.464}Mg_{0.022})_2SiO_4$, containing both Fe^{2+} and Mn^{2+} ions in $M(1)$ positions, is slightly larger (2.168 Å) than that in fayalite (2.158 Å). Furthermore, in the roepperite $(Mn_{0.650}Mg_{0.172}Zn_{0.114}Fe_{0.064})_2SiO_4$, the $M(1)$–O(3) distances are smaller (2.190 Å) than those in fayalite (2.230 Å); and the $M(1)$–O(1) and $M(1)$–O(2) distances, which are comparable (2.122 Å) in fayalite, are dissimilar (2.148 Å and 2.106 Å) in the roepperite structure. These results show that the true symmetry of the $M(1)$ site is lower than the assumed D_{4h} symmetry, which accounts for the discrepency between predicted and measured configurations of the $M(1)$ sites of manganiferous olivines.

Site Populations in the Olivine Structure

The polarized spectra of olivines show that it is possible to distinguish between Fe^{2+} ions in the $M(1)$ and $M(2)$ positions of the olivine structure. Furthermore, the reduced intensity of band II relative to bands I and III in the γ spectra of manganiferous olivines shows qualitatively that cation ordering occurs in the fayalite-tephroite series. Since band II is attributed to Fe^{2+} ions in $M(1)$ positions, the spectra indicate that

Mn^{2+} ions favor the $M(2)$ positions and that Fe^{2+} ions are enriched in the $M(1)$ positions.

The proportions of Fe^{2+} ions in the $M(1)$ and $M(2)$ positions, n_1/n_2, may be estimated quantitatively from the area ratios of component Gaussian curves in the resolved crystal field spectra. Thus,

$$A_1/A_2 = Cn_1/n_2$$

where A_1 and A_2 are the areas under absorption bands originating from Fe^{2+} ions in the $M(1)$ and $M(2)$ positions, respectively, and C is a constant. The constant C may be evaluated from the area data of one standard olivine for which the ratio n_1/n_2 is known. On the assumption that C is constant over the entire Mg^{2+}–Fe^{2+} and Fe^{2+}–Mn^{2+} composition range, the site populations of all Fe^{2+} olivines may be determined from the areas of component Gaussian absorption bands in, for example, the γ polarized spectra.

Since Fe^{2+} ions completely fill all available cation sites in Fe_2SiO_4, the crystal field spectra of pure fayalite must contain contributions from equivalent amounts of Fe^{2+} ions in the $M(1)$ and $M(2)$ positions. No pure fayalite was available in the present study. However, curve resolution of several γ spectra of specimen 10, $(Fe_{1.92}Mn_{0.06}Ca_{0.01}Mg_{0.01})SiO_4$, and specimen 11, $(Fe_{1.96}Mn_{0.03}Ca_{0.01})SiO_4$, gave identical and reproducible area data. Thus, the average areas obtained from eleven spectra of specimen 10 and six spectra of specimen 11 measured on Cary spectrophotometers at Berkeley, Cambridge and Ottawa are

band I : mean 23.5%; range 22.5–25.0%
band II : mean 44.0%; range 42.5–45.5%
band III: mean 32.5%; range 31.0–33.5%

Specimens 10 and 11 contain significant amounts of Ca^{2+} and Mn^{2+} ions, and available evidence suggests that these ions occupy preferentially the $M(2)$ positions of the olivine structure. In order to evaluate C it was assumed that all the Ca^{2+} and Mn^{2+} ions are located in the $M(2)$ positions of these fayalites, leading to reduced amounts of Fe^{2+} ions in these positions relative to the $M(1)$ positions. Thus, the ratios n_1/n_2 for specimens 10 and 11 are assumed to be 0.99/0.93 and 1.00/0.96, respectively.

By taking the average area of bands I and III to be proportional to the amount of Fe^{2+} ions in the $M(1)$ positions, constant C was evaluated from

$$A_1/A_2 = \tfrac{1}{2}(A_{\mathrm{I}} + A_{\mathrm{III}})/A_{\mathrm{II}} = Cn_1/n_2$$

This led to values of C of 0.60 and 0.61, respectively.

Alternatively, on the assumption that Fe^{2+} ions are equally distributed

TABLE 4. DISTRIBUTIONS OF Fe^{2+} IONS IN OLIVINES FROM THE CRYSTAL FIELD SPECTRA

Specimen Number	Fe^{2+} p.f.u.	$Mn^{2+}+Ca^{2+}$ p.f.u.	Areas			Fe^{2+} in $M(1)$	Fe^{2+} in $M(2)$
			Band I	Band II	Band III		
1	0.168	0.002	24.0	46.0	30.0	0.08	0.08
2	0.246	0.014	24.5	47.0	28.5	0.12	0.13
3	0.322	0.008	22.5	48.0	29.5	0.15	0.17
4	0.858	0.010	23.0	45.5	31.5	0.43	0.43
5	1.150	0.130	26.0	42.0	32.0	0.61	0.54
6	1.406	0.022	23.5	46.0	30.5	0.68	0.71
7	1.448	0.146	25.5	42.5	32.0	0.76	0.69
8	1.560	0.040	23.0	45.0	32.0	0.78	0.78
9	1.702	0.030	24.5	45.5	30.0	0.84	0.86
10	1.922	0.068	23.5	44.0	32.5	0.99[a]	0.93[a]
11	1.958	0.040	23.5	44.0	32.5	1.00[a]	0.96[a]
12	1.38	0.528	31.0	36.5	32.5	0.81	0.57
13	0.830	1.00[b]	32.0	31.0	37.0	0.52	0.29
14	0.622	1.354	50.0	29.0	21.0	0.41	0.21

[a] Assumed distribution.
[b] Includes 0.172 Zn^{2+}.

over the $M(1)$ and $M(2)$ positions of each fayalite, the value of C is 0.64. On the other hand, calculations based on the widest ranges of area data for bands I, II and III lead to values of C between 0.67 and 0.58. Taking the relative merits of all these factors into account, the best value of C is considered to be 0.61.

Having obtained a value for C, the ratios n_1/n_2 may be calculated for other Fe^{2+} olivines from the area data in the resolved γ spectra. The results of these calculations are summarized in Table 4. Columns 4, 5 and 6 of this table list the average areas obtained from at least four resolved γ spectra of each olivine. These area data are reproducible to within five percent of the figures quoted. The amounts of Fe^{2+} ions in the $M(1)$ and $M(2)$ positions are given in the last two columns of Table 4.

Although the site populations in Table 4 have an accuracy of between 5 and 10 percent, the data suggest that in olivines containing negligible amounts of Mn^{2+} and Ca^{2+} ions, the Fe^{2+} ions are equally distributed over the $M(1)$ and $M(2)$ positions of the olivine structure. However, there is a consistent trend towards slight relative Fe^{2+} enrichment in the $M(2)$ positions, but in no specimen does the amount of iron in this position exceed 51 percent of the total Fe^{2+} ion content. These results may be compared with recent refinements of the olivine structure which show no evidence of ordering of Mg^{2+} and Fe^{2+} ions (Birle *et al.*, 1968; Hanke, 1965). In those Mg^{2+}–Fe^{2+} olivines containing appreciable amounts of

Mn^{2+} ions (specimens 6 and 7) there is a consistent trend towards slight Fe^{2+} ion enrichment in $M(1)$ positions.

In the Fe^{2+}–Mn^{2+} olivines there is significant enrichment of Fe^{2+} ions in $M(1)$ positions, indicating that Mn^{2+} ions occupy preferentially the $M(2)$ positions. However, the data for specimen 12, for example, show that all the manganese does not enter the $M(2)$ positions and that at least 20 percent of the Mn^{2+} ions must occupy $M(1)$ positions. These results are in good agreement with those obtained by Gibbs and Brown (personal communication) for the knebelite $(Fe_{1.028}Mn_{0.928}Mg_{0.044})SiO_4$, in which site populations determined from counter data using Finger's RFINE program were estimated to be $M(2) = Mn_{0.633}Fe_{0.367}$; $M(1) = Fe_{0.661}Mn_{0.294}Mg_{0.045}$. No decisive conclusions can be drawn about the site occupancy of Zn^{2+} ions in the roepperite (specimen 13). Iron continues to show relative enrichment in $M(1)$ positions as a result of Mn^{2+} (and Zn^{2+}?) ion preference for $M(2)$ positions, and all the zinc could be accommodated in either or both the $M(1)$ and $M(2)$ positions. These results for the relative enrichment of iron in roepperite differ from those obtained by Gibbs and Brown (personal communication) for the specimen $(Mn_{1.300}Mg_{0.344}Zn_{0.228}Fe_{0.128})SiO_4$, in which site populations were estimated as $M(2) = Mn_{0.868}Fe_{0.085}Zn_{0.047}$ and $M(1) = Mn_{0.432}Mg_{0.345}Zn_{0.180}Fe_{0.043}$.

Interpretation of the Site Population Data. The average metal-oxygen distances in Mg^{2+}–Fe^{2+} olivines show that the $M(2)$ site is slightly larger than the $M(1)$ site. Thus, size criteria would lead to the predicton that larger cations will favor the $M(2)$ positions relative to the $M(1)$ positions (Ghose, 1962; Burns, 1970a). As a result, Mn^{2+} (ionic radius 0.82 Å, Shannon and Prewitt, 1969) and Ca^{2+} (1.00 Å) ions are expected to enter $M(2)$ sites preferentially and lead to Mg^{2+} (0.72 Å) and Fe^{2+} (0.77 Å) ion enrichment in $M(1)$ positions. The data in Table 4 for specimens 5 and 7 and the manganiferous olivines (specimens 12, 13 and 14) are in accord with this prediction. Analogous cation distributions based on size criteria have been found in other olivine-type structures (Newnham, Santoro, Pearson and Jansen, 1964; Santoro and Newnham, 1967).

On this basis Fe^{2+} ions might be expected to show a pronounced enrichment over Mg^{2+} ions in $M(2)$ positions of the forsterite-fayalite series. However, the recent refinements to the crystal structure (Birle *et al.*, 1968; Hanke, 1965) and the data in table 4 indicate that the occupancy of Fe^{2+} ions in the $M(1)$ and $M(2)$ positions approaches a random distribution, with only a very small tendency towards relative enrichment in $M(2)$ postions. The absence of a distinct site preference for Fe^{2+} ions in the olivine structure compared to other silicates may be explained by crystal field theory. (Burns, 1970b).

The ground-state electronic configuration of the Fe^{2+} ion in octahedral coordination corresponds to five electrons occupying singly each of the five $3d$ orbitals and the sixth $3d$ electron filling one of the low energy orbitals of the t_{2g} group. This sixth electron induces a crystal field stabilization energy of $\frac{2}{5}\Delta_o$ on the Fe^{2+} ion in octahedral coordination. The crystal field splitting parameter Δ is inversely proportional to the fifth power of the metal-oxygen distance, suggesting that

$$\Delta_{M(2)} < \Delta_{M(1)}$$

and that the stabilization energy of Fe^{2+} in the larger $M(2)$ site is smaller than that in the smaller $M(1)$ site. Therefore, a simple crystal field criterion would lead to the prediction that Fe^{2+} ions (and other transition metal ions acquiring crystal field stabilization energy) would be enriched in the smaller $M(1)$ site (Burns, 1970a).

However, distortion of the $M(1)$ and $M(2)$ sites from octahedral symmetry leads to the stabilization of one or two of the t_{2g} orbitals (Figure 5b&c). By filling one of these low energy orbitals the sixth $3d$ electron of Fe^{2+} induces an additional crystal field stabilization energy on the cation. Although the nature of the distortions of the $M(1)$ and $M(2)$ coordination sites differ in detail (Figure 1), the energy level diagrams shown in Figure 5 suggest and calculations show (Burns, 1970b, p. 83) that the resolution of $3d$ orbitals of iron and the overall stabilization energy may be comparable in the two coordination sites of forsteritic olivines.

It is noteworthy that the olivine structure differs from those of other ferromagnesian silicates by having two moderately distorted six-coordinate sites. The ordering of Fe^{2+} ions found in pyroxene and amphibole structures may be correlated with the preference of iron for the most distorted octahedral sites in these structures (Burns, 1968).

Conclusions

The present paper illustrates further applications of polarized absorption spectral measurements to crystal chemical problems of silicate minerals. First, the compositional variations of absorption bands form the basis of another olivine composition determinative curve, from which the Fe_2SiO_4 content of unanalysed olivines of the forsterite-fayalite series may be estimated. The maxima of all absorption bands in the polarized spectra move to longer wavelengths with increasing Fe_2SiO_4 component in the olivine. However, since Mn^{2+} ions also produce shifts of absorption maxima to longer wavelengths, the determinative curves are best suited to olivines containing negligible manganese.

Second, contributions from Fe^{2+} ions in each of the six-coordinate posi-

tions may be distinguished in the crystal field spectra of olivines. Therefore, areas under absorption bands can be used to estimate Fe^{2+} site populations in the olivine structure. In the forsterite-fayalite series, Fe^{2+} ions are almost equally distributed over the $M(1)$ and $M(2)$ positions of the olivine structure, but there is a suggestion that Fe^{2+} ions show very slight relative enrichment in $M(2)$ positions. In manganiferous olivines, Fe^{2+} ions are concentrated in $M(1)$ positions through the preference of the larger Mn^{2+} ions for the larger $M(2)$ coordination site. As a result, small amounts of Mn^{2+} (and Ca^{2+}) ions in Mg^{2+}–Fe^{2+} olivines lead to slight relative enrichment of Fe^{2+} ions in $M(1)$ positions instead of $M(2)$ positions.

Third, energy level diagrams for each Fe^{2+} ion in the olivine structure may be calculated from the positions of absorption bands. The site populations of the Fe^{2+} ion in the olivine structure may be interpreted by crystal field theory.

Fourth, measurements of polarized absorption spectra enable the concepts of color and pleochroism to be defined more rigorously. The appearance of absorption bands outside or on the fringes of the visible region produce pale green or yellow colors in Mg^{2+}–Fe^{2+} olivines. However, the polarized spectra show that olivines are strongly pleochroic, but the effect is not seen under the microscope because radiation in the near infrared is affected. In tephroites, even though absorption bands occur in the visible region, the very low intensity of the bands and small differences in the polarized spectra lead to the absence of color and pleochroism in these minerals.

Therefore, the Fe_2SiO_4 content, Fe^{2+} site populations, electronic energy levels and pleochroic scheme may be determined from one set of polarized absorption spectra of an olivine mineral.

Note Added in Proof

After this manuscript was submitted, other papers have been published which describe optical spectral measurements of olivines at elevated temperatures and pressures. These include:

Aronson, J. R., L. H. Bellotti, S. W. Eckroad, R. K. McConnell, and P. C. Von Thüna (1970) Infrared spectra and radiative thermal conductivity of minerals at high temperatures. *J. Geophys. Res.*, **75**, 3443–3456.

Pitt, G., and D. C. Tozer (1970) Optical absorption measurements on natural and synthetic ferromagnesian minerals subjected to high pressures. *Phys. Earth Planet. Interiors*, **2**, 179–188.

Acknowledgments

The spectral measurements were commenced at Berkeley, continued at Cambridge and completed at Ottawa when the author was a visiting research scientist at the Mines Branch, Department of Energy, Mines and Resources, during the summer of 1969. At Berkeley,

thanks are due to Professors W. S. Fyfe and A. Pabst for helpful advice and discussion. I wish to thank Professor W. A. Deer and Professor Lord Todd for making facilities available to me in the Deaprtment of Mineralogy and Petrology and University Chemical Laboratories, respectively, at Cambridge. I appreciate the invitation, facilities and helpful suggestions offered to me by Dr. E. H. Nickel at Ottawa. Dr. D. C. Harris generously performed electron microprobe measurements on some of the specimens. Mr. G. H. Faye, Profesor G. V. Gibbs, and Dr. G. E. Brown kindly read the draft manuscript and offered many valuable criticisms and unpublished data. I wish to thank several mineralogists for offering me olivine specimens for this and other studies. Professor A. Pabst, Dr. S. O. Agrell, and Professor E. A. Vincent made available specimens and petrographic thin sections from collections and Berkeley, Cambridge and Oxford, while Dr. B. Mason, Professor C. S. Hurlbut, Jr., and Professor Th. G. Sahama donated various rare and unusual olivines.

References

Balcan, A. S., and H. G. Drickamer (1959) Effect of pressure on the spectra of olivine and garnet. *J. Appl. Phys.* **30,** 1446–1447.

Bancroft, G. M., R. G. Burns, and R. A. Howie (1967) Determination of the cation distribution in the orthopyroxene series by the Mössbauer effect. *Nature,* **213,** 1221–1223.

———, ———, and A. G. Maddock (1967a) Determination of cation distribution in the cummingtonite-grunerite series by Mössbauer spectra. *Amer. Mineral.* **52,** 1009–1026.

———, ———, and ——— (1967b) Applications of the Mössbauer effect to silicate mineralogy. Part 1. Iron silicates of known crystal structures. *Geochim. Cosmochim. Acta,* **31,** 2219–2246.

Belov, N. V., E. N. Belova, N. H. Andrianova, and P. F. Smirnova (1951) Determination of the parameters in the olivine (forsterite) structure with the harmonic three-dimensional synthesis. Dokl. Akad. Nauk SSSR, **81,** 399–402.

Birle, J. D., G. V. Gibbs, P. B. Moore, and J. V. Smith (1968) Crystal structures of natural olivines. *Amer. Mineral.* **53,** 807–824.

Bragg, W. L., and G. B. Brown (1926) Die Struktur des Olivins. *Z. Kristallogr.* **63,** 538–556.

Brown, G. B., and J. West (1927) The structure of monticellite ($MgCaSiO_4$). *Z. Kristallogr.* **66,** 154–161.

Burns, R. G. (1965) Electronic spectra of silicate minerals. Applications of crystal field theory to aspects of geochemistry. Ph.D. Dissertation Univ. Calif., Berkeley, Calif.

——— (1966) Apparatus for measuring polarized absorption spectra of small crystals. *J. Sci. Instrum.* **43,** 58–60.

——— (1968) Crystal field phenomena and iron enrichments in pyroxenes and amphiboles. *In International Mineralogical Association Papers and Proceedings of the Fifth General Meeting, Cambridge, England, 1966.* Mineralogical Society, London, p. 170–183.

——— (1969) Optical absorption in silicates. *In* Runcorn, S. K., ed., *The Application of Modern Physics to the Earth and Planetary Interiors.* J. Wiley and Sons, New York.

——— (1970a) Site preferences of transition metal ions in silicate crystal structures. Intern. Mineral. Assoc., 6th Gen. Meeting, Prague. *Chem. Geol.* **5,** 275–283.

——— (1970b) *Mineralogical Applications of Crystal Field Theory.* Cambridge University Press, England.

——— and R. G. J. Strens (1967) Structural interpretation of polarized absorption spectra of Al-Fe-Mn-Cr epidotes. *Mineral. Mag.* **36,** 204–226.

Clark, S. P., Jr. (1957) Absorption spectra of some silicates in the visible and near infrared. *Amer. Mineral.* **42,** 32–42.

DEER, W. A., R. A. HOWIE, AND J. ZUSSMAN (1963) *Rock-Forming Minerals, vol.* 1, Longmans, England.

DUKE, D. A., AND J. D. STEPHENS (1964) Infrared investigation of the olivine group minerals. *Amer. Mineral.* **49,** 1388–1406.

EIBSCHÜTZ, M., AND GANIEL, U. (1967) Mössbauer studies of Fe^{2+} in paramagnetic fayalite. *Solid State Commun.* **5,** 267.

FARRELL, E. F., AND R. E. NEWNHAM (1965) Crystal field spectra of chrysoberyl, alexandrite, peridot and sinhalite. *Amer. Mineral.* **50,** 1972–1981.

FUKAO, Y., H. MIZUTANI, AND S. UYEDA (1968) Optical absorption spectra at high temperatures and radiative thermal conductivity of olivines. *Phys. Earth Planet. Interiors,* **1,** 57–62.

FURLANI, C. (1957) Spettri di assorbimento di complessi electrostatic del Fe^{2+}. *Gazz. Chim. Ital.* **87,** 371–379.

GHOSE, S. (1961) The crystal structure of a cummingtonite. *Acta Crystallogr.* **14,** 622–627.

——— (1962) The nature of Mg^{2+}–Fe^{2+} distribution in some ferromagnesian silicate minerals. *Amer. Mineral.* **47,** 388–394.

——— (1965) Mg^{2+}–Fe^{2+} order in an orthopyroxene $Mg_{0.93}Fe_{1.07}Si_2O_6$ *Z. Kristallogr.* **122,** 81–99.

———, AND S. HAFNER (1967) Mg^{2+}–Fe^{2+} distribution in metamorphic and volcanic orthopyroxenes. *Z. Kristallogr.* **125,** 1–6.

GIBBS, G. V., P. B. MOORE, AND J. V. SMITH (1963) Crystal structures of forsterite and hortonolite varieties of olivine (abstr.) *Geol. Soc. Amer. Spec. Pap.* **76,** 66.

GRUM-GRZHIMAILO, S. V. (1958) The color of idiochromatic minerals. *Zap. Vses. Mineral. Obshch.* **87,** 129–150.

——— (1960) The color of diamond accessory minerals. *Mater. Vses. Nauch. Issled., Geol. Inst.* **40,** 57–64.

HANKE, K. (1956) Beitrag zu Kristallstrukturen vom Olivin-Typ. *Contrib. Mineral. Petrology,* **11,** 535–558.

———, AND J. ZEEMAN (1963) Verfeinerung der Kristallstruktur von Olivin. *Naturwissenschaften,* **50,** 91.

HURLBUT, C. S., JR. (1961) Tephroite from Franklin, New Jersey. *Amer. Mineral.* **46,** 549–591.

KEESTER, K. L., AND W. B. WHITE (1968) Crystal-field spectra and chemical bonding in manganese minerals. *In International Mineralogical Association Papers and Proceedings of the Fifth General Meeting, Cambridge, England. 1966.* Mineralogical Society, London p. 22–35.

KONDO, H., AND S. MIYAHARA (1963) Magnetic properties of some synthetic olivines. *J. Phys. Soc. Japan,* **18,** 305.

KUNDIG, W., J. A. CAPE, R. H. LUNDQUIST, and G. CONSTABARIS (1967) Some magnetic properties of Fe_2SiO_4 from 4°K to 300°K. *J. Appl. Phys.* **3,** 947.

LEHMANN, H., H. DUTZ, AND M. KOLTERMANN (1961) Ultrarotspektroskopische Untersuchungen zur Mischkristallreihe Forsterite-Fayalite. *Ber. Deut. Keram. Ges.,* **38,** 512–514.

MASON, B. (1959) Tephroite from Clark Peninsula, Wilkes, Land, Antarctica. *Amer. Mineral.* **44,** 428–430.

MUIR, I. D. (1954) Crystallization of pyroxenes in an iron-rich diabase from Minnesota. *Mineral. Mag.* **30,** 376.

NAGATA, T., T. YUKUTAKE, AND S. UYEDA (1957) On magnetic susceptibility of olivine. *J. Geomagn. Geoelec.,* **1957,** 51–56.

NEWNHAM, R. E., R. SANTORO, J. PEARSON, AND C. JANSEN (1964) Ordering of Fe and Cr in chrysoberyl. *Amer. Mineral.* **49,** 427–430.

O'DANIEL, H., AND L. TSCHEISCHWILLI (1964) Strukturuntersuchungen an Tephroite Mn_2SiO_4, Glaukochroite $(MnCa)_2SiO_4$, und Willemite Zn_2SiO_4. *Z. Kristallogr.*, **105,** 273–278.

ONKEN, H. (1965) Verfeinerung der Kristallstruktur von Monticellit. *Tschermaks Mineral. Petrogr. Mitt.*, **10,** 34–44.

SAHAMA, TH. G., AND K. HYTÖNEN (1957) Kirschsteinite, a natural analogue to synthetic iron monticellite, from the Belgian Congo. *Mineral. Mag.* **31,** 698–699.

SANTORO, R. P., AND R. E. NEWNHAM (1967) Antiferromagnetism in $LiFePO_4$. *Acta Crystallogr.* **22,** 344–347.

———, ———, AND S. NOMURA (1966) Magnetic properties of Mn_2SiO_4 and Fe_2SiO_4. *J. Phys. Chem. Solids*, **27,** 655–666.

SHANKLAND, T. J. (1969) Transport properties of olivines. *In* S. K. Runcorn, ed., *The Application of Modern Physics in the Earth and Planetary Interiors.* John Wiley and Sons, New York.

SHANNON, R. D., AND C. T. PREWITT (1969) Effective ionic radii in oxides and fluorides. *Acta Crystallogr.* **B25,** 925–946.

SMITH, J. V. (1966) X-ray emission microanalysis of rock-forming minerals. II. Olivines. *J. Geol.* **4,** 1–16.

SPRENKEL-SEGEL, E. L., AND S. S. HANNA (1964) Mössbauer analysis of iron in stone meteorites. *Geochim. Cosmochim. Acta*, **20,** 1913–1931.

TARTE, P. (1963) Etude infra-rouge des orthosilicates et des orthogermantes. II. Structures du type olivine et monticellite. *Spectrochim. Acta*, **19,** 25–27.

VINCENT, E. A., J. A. V. DOUGLAS, AND M. G. BOWN (1964) Note on the revised compositions of two olivines from the Skaergaard intrusion, East Greenland. *Amer. Mineral.* **49,** 805–806.

WHITE, R. W. (1965) *Ultramafic Inclusions in Basalitic Rocks From Hawaii.* Ph.D. Dissertation, Univ. Calif., Berkeley, Calif.

WHITE, W. B., AND K. L. KEESTER (1966) Optical absorption spectra of iron in the rock-forming silicates. *Amer. Mineral.* **51,** 774–791.

——— AND ——— (1967) Selection rules and assignments for the spectra of ferrous iron in pyroxenes. *Amer. Mineral.* **52,** 1508–1514.

Manuscript received, February 2, 1970; accepted for publication, April 2, 1970.